Journal of MATERIALS RESEARCH

Article
DOI:10.1557/s43578-020-00003-6

MULTISCALE MATERIALS MODELING OF INTERFACE-MEDIATED THERMOMECHANICAL BEHAVIOR

FOCUS ISSUE

Extension of the classical theory for types I and II twinning

J. P. Hirth[1], J. Wang[2,a)]

[1] Green Valley, USA
[2] Mechanical and Materials Engineering Department, University of Nebraska-Lincoln, Lincoln, NE 68588, USA
[a)] Address all correspondence to this author. e-mail: jianwang@unl.edu

Received: 27 August 2020; accepted: 2 November 2020

A plane-displacement diagram showing the four twinning elements, planes and directions, is fundamental to the classical theory of twinning. One aspect of the classical theory of type I and II twinning is shown to be inapplicable when the twin rotation is large. We employ the topological model with certain nonlinear characteristics to deduce a modified set of twinning elements. For twinning associated with a small rotation, both the classical theory and the topological model for type I and II twinning are shown, which give the same set of twinning elements. However, only the topological model is applicable for the large rotation case. As for the classical model, the twin plane in the type II twinning case is irrational unless it, and the type I twin is compound. Often, this irrational plane is close to a low-index orientation for a given orientation relationship. Then it can be favorable for the interface to break up into low-index, rational facets, separated by disconnections. This occurs without changing the orientation relationship. We apply the topological model to describe both the irrational type II twins and faceting in NiTi. The results agree with TEM observations.

Introduction

As reviewed by Hardouin Duparc [1], the basic elements for twinning originated with Mügge [2] and described macroscopic twins in minerals. Cahn [3] in a study of twinning in uranium, considered a unit transformation volume, and related the twinning elements to the characteristics of what we now call twinning disconnections (TDs) in the topological model (TM) [4–6]. As reviewed in [7], the Cahn model provided an interpretation of the twin structure and TDs in terms of dislocation Burgers vectors and, implicitly, step heights. Also, the motion of the TDs provided the mechanism for twin growth. The full classical model for the crystallography of twinning was developed later to complete the classical theory of twinning [8, 9]. The crystallographic model provided matrix relations to predict possible twin planes and directions. The classical model has been most successful in describing many examples of K_1 and $\boldsymbol{\eta}_1$ for type I twinning. Forms of twinning include type IC as the most common form and type IIC as the next most common. We designate these with C for classical, because we show that they are special cases of more general types that share the same mechanism. Instead of the historical representation of the twinning elements, K_1 and K_2 for planes, $\boldsymbol{\eta}_1$ and $\boldsymbol{\eta}_2$ for directions, as in [1–7], we use a modified Frank notation [10] for the twinning elements $k_1 = K_1, k_2 = K_2, \boldsymbol{\chi}_1 = \boldsymbol{\eta}_1$, and $\boldsymbol{\chi}_2 = \boldsymbol{\eta}_2$, for type I twins, and $k_1 = K_2, k_2 = K_1, \boldsymbol{\chi}_1 = \boldsymbol{\eta}_2$, and $\boldsymbol{\chi}_2 = \boldsymbol{\eta}_1$ for type II twins. These are useful since k_1 is always the glide plane (the TM does not apply unless there is such a glide plane). For both type IC and type IIC, k_1 and $\boldsymbol{\chi}_2$ are rational, and k_2 and $\boldsymbol{\chi}_1$ are irrational. If all four elements are rational, the twin is called a compound twin.

The characteristics of a TD determine whether it is a feasible twinning defect, with respect to both self-energy and activation energy for motion. For type IC twinning, The TD was defined as a disconnection in order to emphasize the importance of the step height and as an analog of similar defects in phase transformations [11]. TDs are line defects, characterized by the step height h and the Burgers vector $\boldsymbol{b}_g$ describing the dislocation content. In the topological model (TM), the step height h and the corresponding Burgers vector $\boldsymbol{b}_g$ are defined in a coherent dichromatic pattern (CDP), the superposition of the matrix and twin with coincidence on the twin plane, and a common origin. In the CDP, the vector $\boldsymbol{b}_g$ is the difference between rational vectors $\boldsymbol{t}_M$ and $\boldsymbol{t}_T$ for the matrix and twin, respectively. More

recently, the mechanism of type II twinning was outlined [5], and developed in detail in [12, 13]. In this case, TDs move on $k_1 = K_2$ planes and accumulate in a tilt wall, accompanied by partitioning of the rotations to both the matrix and twin, creating symmetrical tilt across the twin boundary [12, 13]. The process can be viewed as the creation of a dislocation array with long-range stresses that relaxes by interface rotation.

On the basis of these mechanisms, we analyze the twinning elements and structures of the twins. We distinguish between the classical models and the TM, which includes certain nonlinear characteristics. We treat type II twins in NiTi as an example. Finally, we describe the mechanism and structure of the formation of low-index, rational facets on the type II twin boundaries.

Type I and IC twins

For type I twins, a source of mobile disconnections operates on the (rational) k_1 plane, eventually generating a macroscopic twin. The type IC mechanism, reviewed in [6, 12], is summarized in Fig. 1a, showing the twinning elements and the twin angle α_C. The classical diagram is a plane-displacement engineering shear diagram, displacing a circle to an ellipse by the vector $\boldsymbol{u}$ at a distance h above the origin [8, 9, 12]. The classical displacement is called the "shear" $\boldsymbol{s}$, which is unfortunate in that it implies that $\boldsymbol{s}$ is the shear strain. The engineering shear strain is $e = u/h = \tan 2\alpha_C$. For a type II twin, symmetry requires that the displacements have a mirror symmetry plane normal to y or have the x axis as a 2-fold rotation axis. For the classical case, this is implied by setting the shear angle γ_{xy} equal to $2\alpha_C$ as in Fig. 1a. This is precise only in the limit of infinitesimal strain. In order to achieve actual displacement symmetry, there must be a different state of shear strain as in Fig. 1b: a compression along y and an equal measure extension along x, Fig. 1b. More conveniently for the analysis of twin characteristics, as in [13], these displacements can be viewed alternatively as two opposite engineering strains, $\pm e/2 = 0.5u/h = \tan\alpha$, as in Fig. 1c.

In order to connect to TDs, one imagines atom coincidence at the origin and an atom a distance h from the origin shearing by a displacement $\boldsymbol{b}_g$ to a position in k_2'. This produces a shear $e = b_g/h$. The twinning elements are represented in Fig. 2a and the TM version in Fig. 2b. Hence, the twinning angle is

$$\alpha = \tan^{-1}(e/2) = \tan^{-1}(0.5\boldsymbol{b}_g/h). \quad (1)$$

This differs from the linearized classical value as follows:

$$\alpha_C = \frac{1}{2}\tan^{-1}(e) = \frac{1}{2}\tan^{-1}(\boldsymbol{b}_g/h). \quad (2)$$

The TM type I supersedes the classical type IC model when e is large. Figure 3 is a plot of the difference $\Delta\alpha = (\alpha - \alpha_C)$ versus α. Practically, the classical model is a good approximation when $\alpha$is less than $\approx 3°$, but there is a significant difference for larger α. The nonlinear model was mentioned in [13] but not quantified because α was small.

In the most general classical case, the vector parallel to $\boldsymbol{\chi}_2$ is a 2' rotation axis. In many high-symmetry cases, the twin plane also has m' mirror symmetry.

Type II and IIC twins

The mechanism for type II twinning entails TDs moving on $k_1 = K_2$ planes and accumulating in a tilt wall, accompanied by partitioning of the rotations to both the matrix and twin, creating symmetrical tilt across the twin boundary [12–14]. This means that the type II twin formation consists of two deformation mechanisms: engineering shear and interface rotation. Here, we extend the TM mechanism as for type I to show similar deviations from the classical model. Figure 4a and b are diagrams for type II twinning analogous to Fig. 2. Glide by $\boldsymbol{b}_g$ on k_1 would produce the same engineering shear e. In this case, the engineering shear partitions to $e/2$ in each crystal. For the most likely situation where unit TDs have step heights equal to the interplanar distance normal to k_1, the engineering shear e cannot actually mechanistically partition because there would be profuse stacking fault formation: with multiple step height disconnections, actual partitioning of e is possible [5, 15]. The mechanism is that perfect lattice dislocations shear and then dissociate into partial dislocations in the k_2 plane. However, the effect of partitioning is that the final configuration is the same as in a hypothetical process where the engineering strains are partitioned. Hence the final twin has partitioned engineering strains, displacements, crystal structure, and rotations. The results are the same as for type IIC provided that e is small, Eq. (2) applies and the twinning angle is α_C: type IIC. The $\boldsymbol{t}_M$ and $\boldsymbol{t}_T$ vectors rotate into conjunction and the $\boldsymbol{\chi}_2$ vector is parallel to the rational, common $\boldsymbol{t}$ direction. If e is not small, Eq. (1) applies, and the twinning angle is α: type II. The TM analysis in [12, 13] is accurate except for this angle. *Thus, only when e is small, does the classical model apply. Otherwise, the TM model is applicable.*

The essence of the differences discussed above is that the partitioning of distortions into strains and rotations varies with the rotation of coordinates. For type I, the classical model is exact because there are no such rotations, present for type II, provided that one uses the symmetric configuration of Fig. 1b. There is a rare special large angle case, typified by (111) twins in *fcc* crystals that can also be understood from Fig. 4. For this twin, the angle α is so large, 19.47°, significantly different from $\alpha_C = 17.63°$, that a different {111} plane rotates to become the rational $k_2 = K_1$ plane and the classical model applies. Thus, for *fcc*, without ancillary data such as strain measurements, one cannot tell whether a twin is created by a type IC or type IIC mechanism. Also, for (301) twins in cubic systems, if the

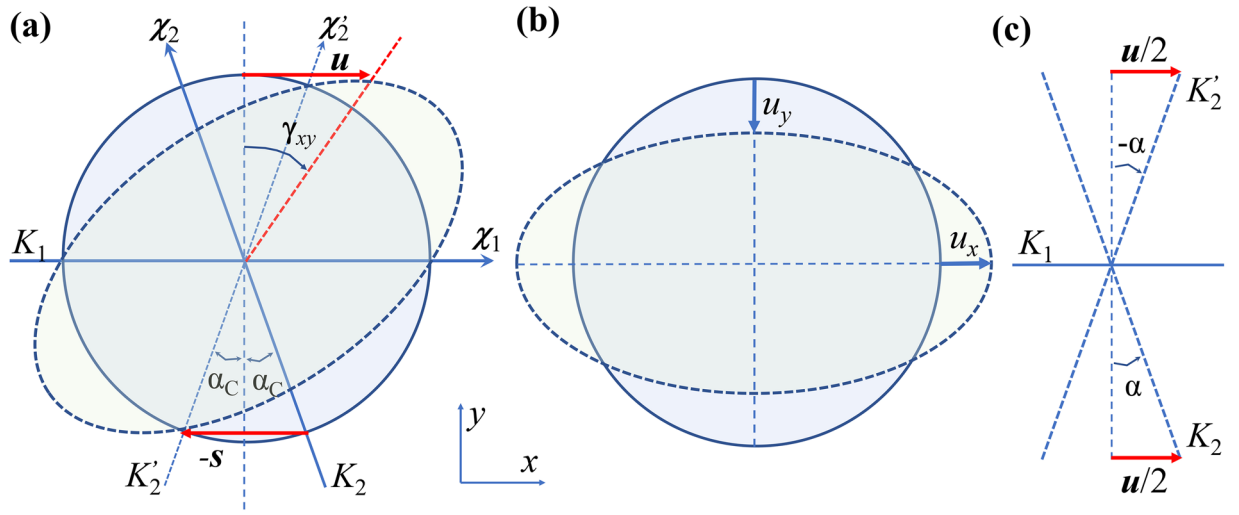

Figure 1: (a) Classical diagram showing the shear of a circle into an ellipse. (b) Symmetric state of shear produced by compression along *y* and extension along *x*. (c) Alternate view of the displacements in (b). One can imagine a positive engineering shear above the twin plane and a negative engineering shear below the twin plane.

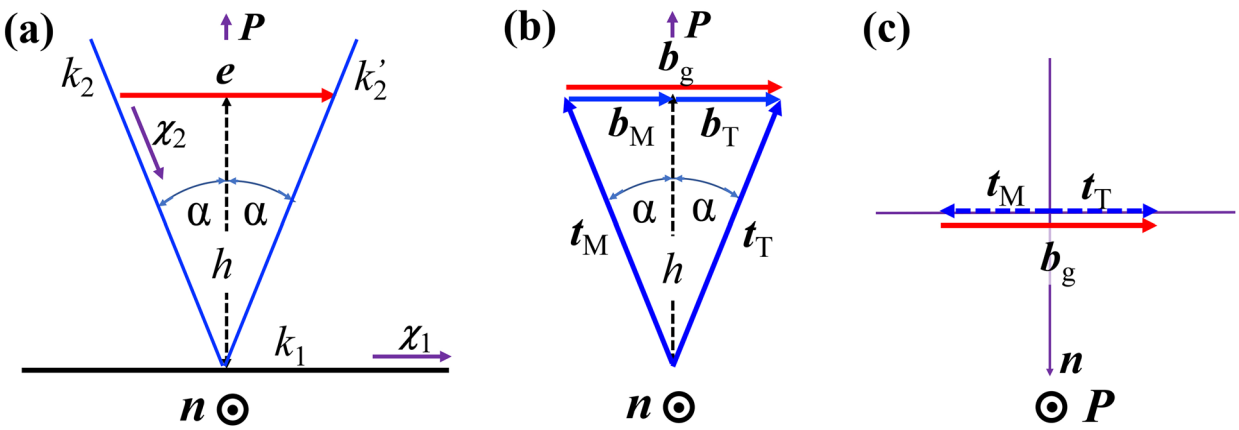

Figure 2: (a) Classical view normal to the plane of distortion showing twinning elements for a type IC twin, those for the twin are denoted with a prime. Engineering shear $\boldsymbol{e}$ on the k_1 plane produces the shear displacement and the characteristic rotation angle α. (b) TM view showing translation vectors $\boldsymbol{t}_M$ and $\boldsymbol{t}_T$ in the dichromatic pattern, the disconnection step height, h, and the partitioned Burgers vectors $\boldsymbol{b}_M$ and $\boldsymbol{b}_T$. (c) Projection along $-\boldsymbol{P}$ for the general case showing that the vectors $\boldsymbol{t}_M$ and $\boldsymbol{t}_T$ lie in the plane of distortion.

conjugate is (103), an engineering shear alone describes type II. This is a consequence of the interdependence of the tensor strain components *ij* and *ji*.

For a complete analysis of twinning, one often needs to consider the shuffling of atoms that are not at lattice sites, [3, 9, 13, 16]. For these, it is useful to describe the superposed lattices in a rotated dichromatic pattern (RDP) [4], or a shifted dichromatic pattern (SDP) [5, 17]. Shuffles are not needed here. We do not discuss them further.

The actual mechanism of type II twinning is shown in Fig. 5, a version of the diagrams in [5, 12, 13]. As indicated, unit TD pairs nucleate and glide on k_1. They accumulate, and the interface rotates into tilt orientation. The Burgers vectors of the tilt dislocations are $\boldsymbol{b}$. The resolved shear stress in the direction of $\boldsymbol{b}_g$ provides a first-order Peach-Koehler force driving the reaction. The unit advance of the step is a rotation equivalent to the motion of a disclination quadrupole [18]. Hence, there are second-order driving forces entailing either the couple stresses doing work when rotation occurs, or a change in strain energy in the anisotropic elastic case when the elastic constant matrix is rotated. The activation energy for motion is influenced by the Peierls barrier for glide and the diffusion-like shuffling required to complete the transformation.

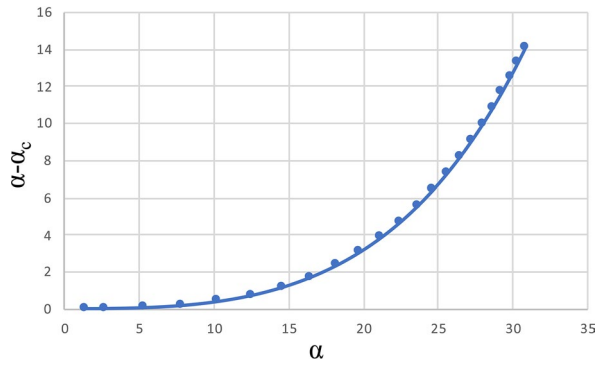

Figure 3: Plot of $\Delta\alpha$ versus α.

Type II twin in NiTi

As an example, the results for NiTi [19] are as follows. NiTi is monoclinic with lattice parameters $a_0 = 0.2885$ nm, $b_0 = 0.4120$ nm, $c_0 = 0.4622$ nm, and $\beta_0 = 96.9°$. Type II twinning in NiTi has been analyzed with the TM modification of the classical theory of twinning [13], entailing the experimental results in [19]. The relevant results and characteristics for NiTi are presented in Table 1.

A three-dimensional CDP is shown in Fig. 6a. The CDP viewed along $-\boldsymbol{P}$ is shown in Fig. 6b, with $\boldsymbol{t}_M = [0\bar{1}1]$, $\boldsymbol{t}_T = [01\bar{1}]_T$. The twin is type II. Figure 6c is a projection along $-\boldsymbol{n}$ of a double height disconnection, selected in accord with the 2' symmetry. It provides the data needed in Eq. (1). The results for the type II and IIC analyses are presented in Table 2. For most parameters, the type II and IIC analyses agree. The only differences are for $\Delta\alpha$ and b. For NiTi, the differences are essentially insignificant. They do serve to indicate that types II and IIC do differ.

Faceting and motion of k_2 twin boundary

When the k_2 boundary is near a low-index, rational plane, faceting can occur [16, 20, 21]. The relevance here is that the most likely faceting occurs for small twin angles where the classical description applies. For example, Knowles [22] suggested the possibility of faceting for the type II twin in NiTi, and such facets were indeed found in an HRTEM study of NiTi [23]. They are also likely for many minerals where the $\boldsymbol{b}_g$ for the TDs tends to be small. An example is labradorite, where such facets were observed for a type II pericline twin [14]. There are different possibilities for motion of TDs causing growth or detwinning of a type II twin depending on step height. In what follows, we discuss the faceting mechanism of the k_2 twin boundary and the reversed or continued motion of a faceted interface.

We first consider the faceting mechanism. For the most general twin boundary, the displacements always have pure tilt symmetry. However, the k_2 boundary is irrational and, relative to the low-index facet, can contain four sets of dislocations, two edge arrays associated with orthogonal tilts and two associated with a twist. This is analogous to the reduced von Mises criterion at a grain boundary [24]. If the screw arrays are orthogonal screws, they are not independent, since, operating together they produce a pure rotation without strain. However, both sets, which could actually be edge or mixed in character [25], must be present to prevent coherency stresses from appearing. There are three independent systems that satisfy the compatibility condition that the *xx*, *yy*, and *xy* strains in forming the boundary are the same in the two crystals when the axes *x* and *y* lie in the boundary, Thus, to remove any one of these sets in producing the facet,

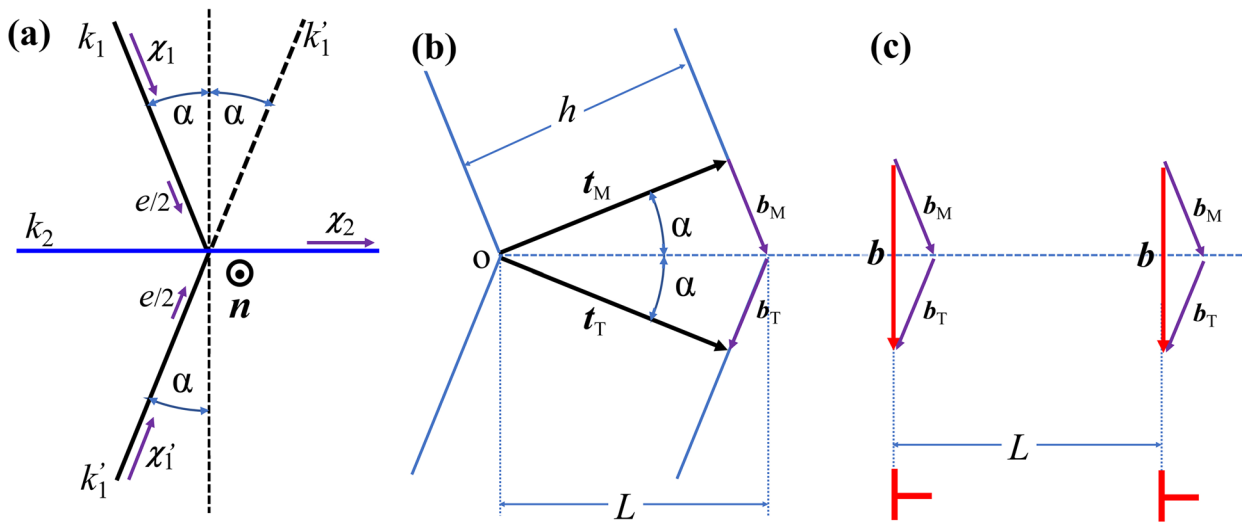

Figure 4: (a) View normal to the plane of distortion for a type II twin with $\boldsymbol{t}_M$ and $\boldsymbol{t}_T$ in the plane of distortion. Partitioned engineering strains produce a type II twin with a rotation angle α and tilt Burgers vector $\boldsymbol{b}$. (b) TM, view showing the partitioned Burgers vectors that sum to the tilt vector $\boldsymbol{b}$ on the twin plane. (c) Details of the tilt dislocation spacing.

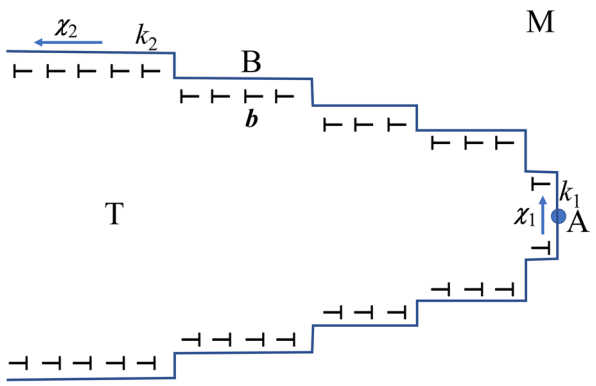

Figure 5: TDs nucleate at A, glide, and accumulate. The Burgers vector rotates into the tilt configuration B, eventually creating the type II twin boundary k_2.

the mechanism is as follows. The atomically spaced dislocations $\boldsymbol{b}$ entail atom-atom overlap and should spontaneously relax into discrete disconnection b_D bounding the low-index terraces: the facets. The net Burgers vector $\boldsymbol{B}$ of the original defects now resides in the disconnection and the removal of the defects leaves coherency dislocations on the facets with a net $\boldsymbol{B}_c$ equal and opposite to $\boldsymbol{B}$, Fig. 7, explicitly demonstrated and simulated in [4].

For a lenticular, type II deformation twin, there are three possible facet surfaces. Mechanistically, the most likely is a facet close to the k_2 plane as in Fig. 7, and we discuss that case first. However, the tip of the twin and large steps on the k_2 plane can form facets close to the k_1 plane: Conversely, large steps on the k_1 plane can form facets close to the k_2 plane: Also, facets could form close to the plane of distortion on portions of that twin where the TDs are in edge orientation. For blocky twins, all three types could bond a relaxed parallelepiped shape [19]. For facets appearing as steps, if the step height is a large multiple mh_0 of the unit step height h_0, with m an integer, then only the process described in [16, 20, 26] is feasible. The riser of the step is equivalent to a disclination dipole, and the advance of the step requires the nucleation and propagation of TDs on the step riser [27].

For NiTi, Fig. 7a shows the dislocation description of the k_2 plane with one tilt dislocation for each intersecting k_1 plane. The interface relaxes to form a low-index terrace (facet) with an orientation close to the k_2 plane, accompanied by partitioning by the mechanism described in [4]. The structure is that of Fig. 7b, a coherent terrace (facet) of size L described by an array of infinitesimal coherency dislocations and disconnections with equal and opposite $\boldsymbol{B}$. As in [4], many interfaces relax in this manner. Since all of the TDs arrive from one side, the structure of Fig. 7c is also possible if there is a constraint to partitioning. In this case the tilt angle would change by the tiny increment $b\cos\alpha/h$, usually negligible. In either case, the long-range distortion rotation field is unchanged, but there are local compensating strains. Faceting in NiTi definitely occurs as observed in [23]. It is precisely of the type in Fig. 7c. Because the normal to the $(11\bar{1}\}$ plane is slightly tilted and twisted relative to $\boldsymbol{\chi}_1$, the equilibrium boundary would also have very widely spaced edge disconnections with lines parallel to $\boldsymbol{\chi}_1$ and Burgers vectors normal to (011). Also, there would be orthogonal screw dislocations with wide spacing L and an in-facet-plane Burgers vector.

TABLE 1: Common characteristics for type I twin.

$\boldsymbol{b}_g$	h (nm)	L (nm) [20]
[0.1693, 0.1075, 0.1075]	0.3066	0.800
e	Plane of shear	$\boldsymbol{N}$
0.280	(– 1, 0.7875, – 0.7875)	[– 1, 0.3598, – 0.3598]

The reversed or continued motion of faceted interface could occur by either of two mechanisms. Once faceting occurs, the boundary is pinned by the intersecting defects. Also, direct motion of the disconnections in Fig. 7 is less likely than that for unit TDs because the large Burgers vector results in a much larger Peierls stress. Hence, the mechanism for either continued growth after unloading and relaxation or for reverse deformation as in shape memory applications is likely the reverse of that in Fig. 5. For NiTi, this is consistent with structural observations and consistent with the similarity of the stress for twinning and detwinning [19].

Alternatively, once the Type II plane is formed, it could conceivably advance by nucleation and motion of glide TDs with Burgers vectors $\boldsymbol{b}_g^{II}$ gliding on k_2 suggested in [28]. In other words, disconnections similar to those in Fig. 7 could translate the k_2 interface. In this regard, as shown in Fig. 8, there is a duality of description of such a disconnection. As shown in Fig. 8a, an atomic distance a of the TD is equivalent to the addition of a disclination quadrupole [23]. This can also be regarded as either unit motion laterally of a disconnection with Burgers vector $\boldsymbol{b}_g^{II}$ and step height h^{II}, the Müllner mechanism [28], or by upward motion of a disconnection with Burgers vector b_g and step height h, the TM mechanism. With the observed spacing $L = 0.800$ nm, the Burgers vector of these glide disconnections would be $\boldsymbol{b}_g^{II} = L\tan\alpha = 0.112$ nm. This is twice $\boldsymbol{b}_g$ so the Peierls stress would be too high for the glide mechanism to operate for NiTi. The Müllner mechanism [28] would apply, for example, to the fcc case mentioned previously.

A recent simulation [19] of the same type II twin in NiTi revealed a twinning mechanism of the second type mentioned above: facets on a blocky twin lying close to the plane of distortion, (011). The TDs on this surface have screw orientation. As demonstrated in [20], these interfaces can recover by the same mechanism as the edge portions. The simulation showed that the breakup of the irrational plane of distortion into {011} facets

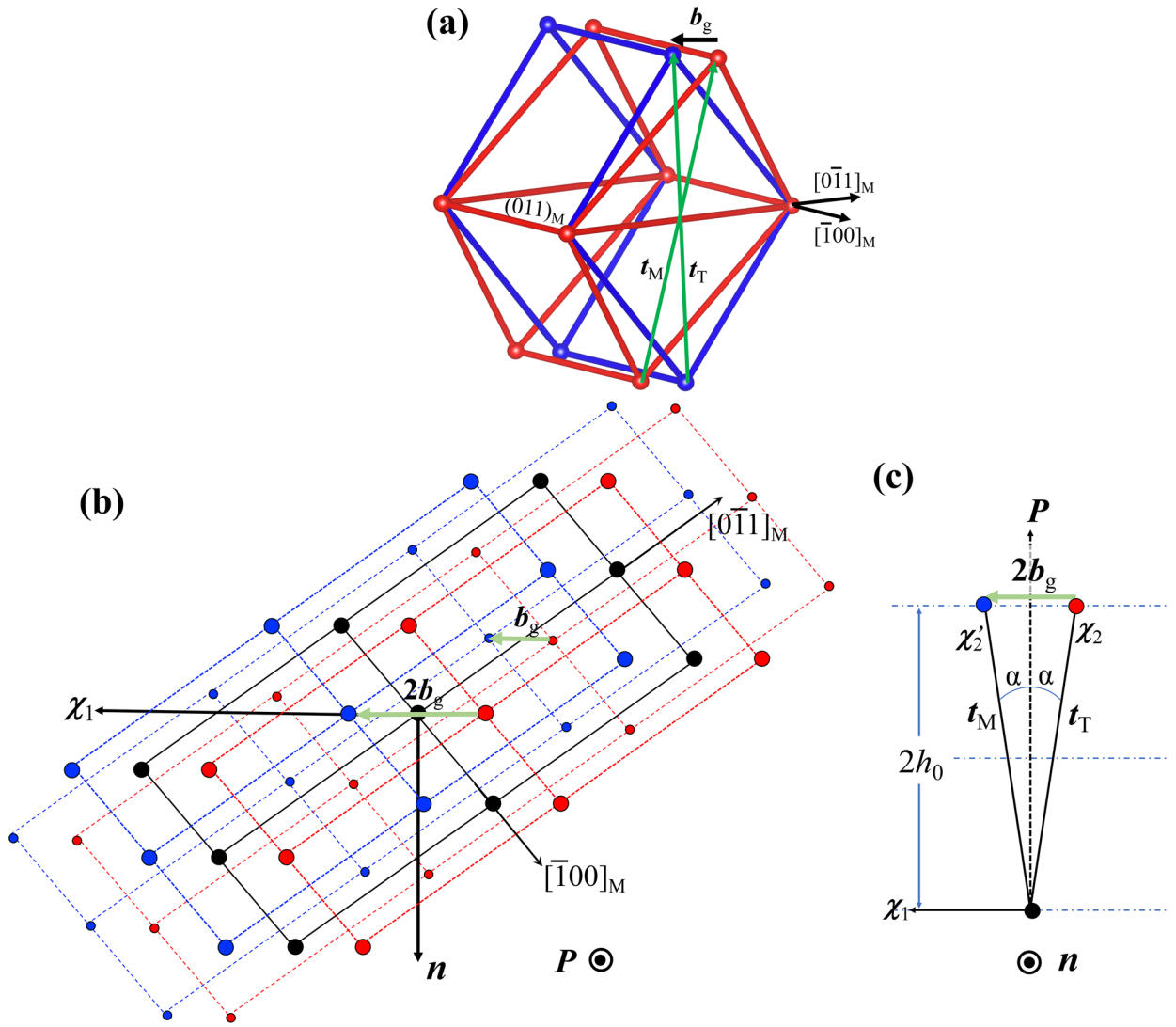

Figure 6: (a) Three-dimensional coherent dichromatic pattern for NiTi. (b) Same pattern viewed along the glide plane normal ***P***. The small red and blue circles represent lattice sites in the first layer and the big red and blue circles are in the 2nd layer. Plane (c) Double height disconnection characteristics in view of DP along −***n***.

TABLE 2: Characteristics and twinning elements for all twin types.

Type	k_1	χ_1	χ_2
IIC	(011)	[1, 0.635, – 0.635]	[011]
II [10]	(011)	[1, 0.635, – 0.635]	[011]
Type	b	k_2	**Twin angle**
IIC	0.082 nm	(0.722, 1, – 1.007)	$\alpha_C = 7.832°$
II [10]	0.086 nm	(0.720, 1, – 1.000)	$\alpha_N = 7.981°$

separated by disconnections with mainly screw components was favorable. In addition, there should be a few disconnections with edge components arising because of the monoclinicity, and a few orthogonal screw dislocations arising from the relaxation [20], but these were not included in the simulation. They observed the Müllner mechanism [28]: the screw disconnections were mobile and could in principle propagate the twin normal to the plane of distortion. However, the presence of orthogonal screw dislocations could pin the structure, so further work might be needed to resolve this issue.

Discussion

For large twinning angles, we have provided an extension of the classical theory for twinning. The source of the difference is a nonlinear plastic effect associated with the difference between engineering and tensor distortion matrices. In systems with smaller twinning angles, the classical theory can be an excellent approximation. However, for small twinning angles, the resultant structure can recover to a faceted configuration with

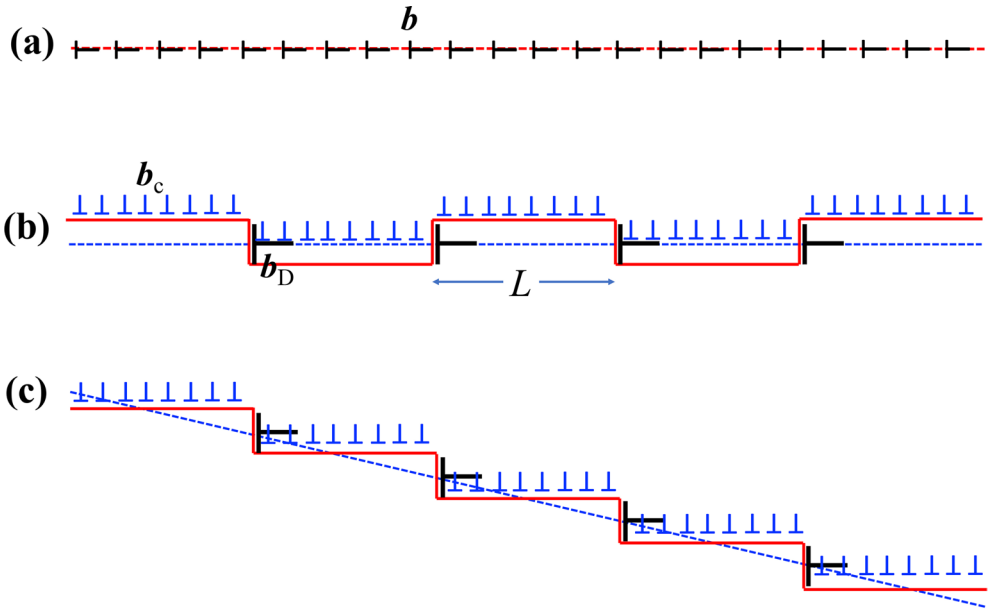

Figure 7: Illustration of the faceting process. (a) Irrational twin plane with atomically spaced dislocations. (b) Relaxation into coherent terraces with the origin of the coherency strains represented by coherency dislocations, separated by partitioned disconnections. (c) Equivalent of (b) but with facets separated by disconnections with a single step direction.

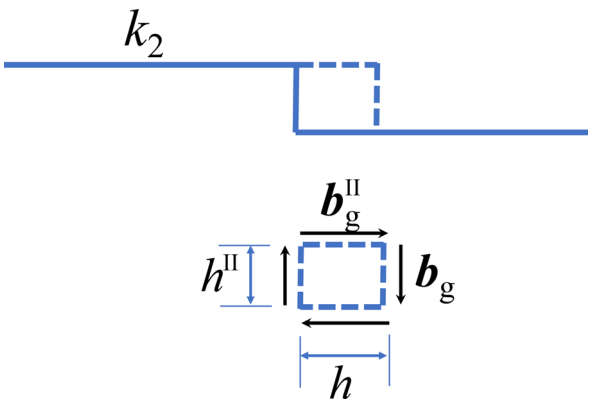

Figure 8: Two equivalent interpretations of the advance of a TD on the k_2 plane.

little cost in surface energy. Analysis shows that such faceting is favored for type II deformation twins in NiTi. The facets are on planes with orientations close to the k_2 plane. The facet configuration agrees with HRTEM observations of recovered type II deformation twins in NiTi. We show that facets can also form in recovered type II planes on large step risers that are close in orientation to a k_1 plane and to large step risers that are close to the plane of distortion. All three types of facets can form on blocky, nominally equiaxed twins.

Summary

We have compared the twinning elements as deduced from the classical model and the topological model for both type I and II twinning. For twinning with a large rotation angle, the topological model is more accurate because nonlinear characteristics of the engineering shear strain are included. For the irrational k_2 twin boundary associated with type II twinning, we propose a possible relaxation mechanism to form low-index, rational terraces (facets) separated by disconnections as observed for type II twins in NiTi. Correspondingly, two possible mechanisms are also proposed for the migration of the faceted twin boundary.

Acknowledgments

This work was financially supported by the U.S. National Science Foundation (NSF) (CMMI-1661686). We thank R.C. Pond for helpful comments.

References

1. O.B.M. Hardouin, Duparc: A review of some elements for the history of mechanical twinning centred on its German origins until Otto Mügge's K1 and K2 invariant plane notation. J. Mater. Sci. **52**, 4182 (2016)

2. O. Mügge, Uber homogene deformationen (einfache schiebungen) an den triklinen doppelsalzen BaCdCl4.4aq. Neues Jahrbuch für Mineral. Geol. Palaeontol. Beilage. **6**, 274 (1889)
3. R.W. Cahn, Plastic deformation of alpha-uranium; twinning and slip. Acta Metall. **1**, 49 (1953)
4. J.P. Hirth, R.C. Pond, R.G. Hoagland, X.Y. Liu, J. Wang, Interface defects, reference spaces and the Frank-Bilby equation. Prog. Mater. Sci. **58**, 749 (2013)
5. J.P. Hirth, J. Wang, C.N. Tomé, Disconnections and other defects associated with twin interfaces. Prog. Mater. Sci. **83**, 417 (2016)
6. A. Ostapovets, A. Serra, Review of non-classical features of deformation twinning in hcp metals and their description by disconnection mechanisms. Crystals (Metals) **10**, 1134 (2020)
7. J.W. Christian, S. Mahajan, Deformation twinning. Prog. Mater. Sci. **39**, 1 (1995)
8. B.A. Bilby, A.G. Crocker, The theory of the crystallography of deformation twinning. Proc. Roy. Soc. A. **288**(1413), 240 (1965)
9. M. Bevis, A.G. Crocker, Twinning shears in lattices. Proc. Roy. Soc. A **304**, 123 (1968)
10. F.C. Frank, Crystal dislocations-elementary concepts and definitions. Phil. Mag. **42**, 809 (1951)
11. J.P. Hirth, R.C. Pond, Steps, dislocations and disconnections as interface defects relating to structure and phase transformations. Acta Mater **44**, 4749 (1996)
12. R.C. Pond, J.P. Hirth, Topological model of type II deformation twinning. Acta Mater **151**, 229 (2018)
13. R.C. Pond, J.P. Hirth, K.M. Knowles, Topological model of type II deformation twinning in NiTi martensite. Phil. Mag. **99**, 1619 (2019)
14. D.Y. Xie, G. Hirth, J.P. Hirth, J. Wang, Defects in deformation twins in plagioclase minerals. Phys. Chem. Minerals **46**, 959 (2019)
15. R. Bullough, The dislocation content of a large angle tilt boundary. Phil. Mag. **5**, 1139 (1965)
16. A. Serra, D.J. Bacon, A new model for 1012 twin growth in hcp metals. Phil. Mag. A **73**, 333 (1996)
17. J.P. Hirth, J. Wang, G. Hirth, A topological model for defects and interfaces in complex crystal structures. Am. Mineral. **104**, 966 (2019)
18. J.P. Hirth, R.C. Pond, J. Lothe, Spacing defects and disconnections in grain boundaries. Acta Mater. **55**, 5428 (2007)
19. A.S.K. Mohammed, H. Sehitoglu, Modeling the interface structure of type II twin boundary in B19' NiTi from an atomistic and topological standpoint. Acta Mater. **183**, 93 (2020)
20. K.M. Knowles, D.A. Smith, The crystallography of the martensitic transformation in equiatomic nickel-titanium. Acta Metall. **29**, 101 (1981)
21. M.Y. Gong, J.P. Hirth, Y. Liu, Y. Shen, J. Wang, Interface structures and twinning mechanisms of twins in HCP metals. Mater. Res. Lett. **5**, 449 (2017)
22. J.W. Christian, Chapter 20—Deformation twinning, in *The Theory of Transformations in Metals and Alloys*, ed. by J.W. Christian (Pergamon, Oxford, 2002)
23. K.M. Knowles, A high-resolution electron microscope study of nickel-titanium martensite. Phil. Mag. **45A**, 357 (1982)
24. Z.L. Xie, Y. Liu, HRTEM study of <011> type II twins in NiTi shape memory alloy. Phil. Mag. **84**, 3497 (2004)
25. P.M. Anderson, J.P. Hirth, J. Lothe, *Theory of Dislocations* (Cambridge University Press, Cambridge, 2017)
26. J.P. Hirth, Stabilization of strained multilayers by thin films. J. Mater. Res. **8**, 1572 (1993)
27. A. Serra, R.C. Pond, D.J. Bacon, Computer Simulation of the structure and mobility of twinning dislocations in hcp metals. Acta Metall. Mater. **39**, 1469 (1991)
28. P. Müllner, Twinning stress of type I and type II deformation twins. Acta Mater. **176**, 211 (2019)